In-Situ Foaming Evolution of Flexible Polyurethane Foam Nanocomposites

M. Mar Bernal, Miguel Angel Lopez-Manchado, Raquel Verdejo*

_____

M.M.B., M.A.L.-M., R.V. Corresponding-Author,
Institute of Polymer Science and Technology, (CSIC); C/ Juan de la Cierva, 3; 28006, Madrid, Spain
Fax: +34 91 564 4853; E-mail: rverdejo@ictp.csic.es

_____

The effect of both as-produced and functionalised CNTs on the polymerisation evolution of water-blown PU foams containing up to 0.3 wt.-% CNTs was studied by *in situ* FT-IR spectroscopy. FT-IR revealed a decrease on the rate of isocyanate conversion as a function of loading fraction for both as-grown and oxidised CNTs. This dependency suggested that the isocyanate conversion at the early stages of the reaction was governed by the kinetic effects imposed by the presence of the CNTs. The onset of microphase separation was accelerated by the addition of functionalised CNTs but not by as-produced CNTs due to the different surface functionalities. Measurements of the foaming viscoelastic properties showed an increase on the storage modulus with the CNT content, which indicated the reinforcement of the foam.

Introduction

Reactive foams are produced as a result of two simultaneous reactions: foaming and polymerisation, water-blown polyurethane foam being one of the largest and most versatile families of these foams. The process presents a liquid-solid phase transition where a liquid mixture, of relatively low molecular weight components, is transformed into the supramolecular architecture of solid foams in under 5 min.[1] Hence, the reaction kinetics of this process has to be well understood in order to control the rates of both the evolution of the gas and the increase in viscosity, since the polymer structure must build up rapidly to support the fragile foam, i.e. to form a stable cellular structure, but not so fast as to stop bubble growth.[2]

The versatility of water-blown PU foams arises not only from the nature and variety of the reaction mixture, but also from the ease of production that enables the development of tailor-made materials over wide range of applications.[3] PU foams are used for their outstanding strength-to-weight ratio, their resilience, and their electrical, thermal, and acoustic insulating properties, amongst other characteristics.[3] PU foam chemistry is based on the reactions of isocyanates with active hydrogen-containing compounds, in particular polyfunctional hydroxyl compounds (or polyols) and water. The reaction of isocyanate with polyol, often termed the *gelling reaction* (**Scheme 1a**), forms urethane linkages, leading to the increase in the molecular weight. Meanwhile, the reaction of isocyanate with water, known as the *blowing reaction* (**Scheme 1b**), forms urea hard segments and carbon dioxide gas from the decomposition of an unstable carbamic acid.[4] As a result of these concurrent reactions a cross-linked network of a segmented block copoly(ether-urethane urea) is blown into a cellular structure by the evolved CO_2 and entrapped air. This reactive processing provides PU foams with a structured morphology stretching over several length scales, from the macroscopic cellular

structure to the microdomains of the segregated urea hard segments and the poly(ether-urethane) soft segments joined by urethane covalent bonds (Scheme 1c). Thus, the final properties of PU foams are strongly dependent upon the reaction kinetics; that is rates of polymerisation, phase separation, solidification, and the inherent connectivity between the phases.

Scheme 1

The foaming evolution of PU has previously been studied through a combination of in-situ FT-IR, rheology and SAXS measurements.[1, 4-8] Real time morphological changes during phase separation are monitored by small angle X-ray scattering experiments.[1, 6] Meanwhile, FT-IR spectroscopy has been used to understand the polymer structure development and the kinetics during foaming.[1, 6, 7] FT-IR enabled monitoring both the sequence of chemical reactions and morphological changes by analysing the decay of isocyanate and the evolution of H-bonded bands. In-situ rheology measurements have provided information on the foaming evolution through changes in the modulus or viscosity profile using a modified parallel-plate rheometer under forced adiabatic conditions.[4, 8, 9] These in-situ studies have established four stages during polyurethane foaming: 1) mixing of the reactants and bubble nucleation and growth by the generation of CO_2 from the water-diisocyanate reaction, 2) evolution of the bubbles to form a packed network and simultaneous formation of urethane and soluble urea moieties leading to the onset of microphase separation of the urea hard segments, 3) increase of the storage modulus due to the formation of an interconnected physical network of hydrogen-bonded hard segments; as the reaction continues the microphase separation is arrested by vitrification and the cell walls open, 4) final curing of the foam where the

storage modulus continues to increase at a slow pace until it stabilises once the vitrification of the hard segments and formation of covalent cross-links is completed.

The inclusion of carbon nanotubes (CNTs) in polymer foams has already been shown to improve their mechanical, electrical and thermal properties.[10-14] Preliminary studies have analysed the effect of nanoclays on polyurethane foaming and have observed an increase of the rates of polymerisation on both vermiculite clay[15] and montmorillonite.[16] Previous works by the authors qualitatively observed an effect of the CNT on the PU foaming reaction[11, 12, 14] and also on the dynamic evolution of silicone reactive foams.[17] It was then suggested that the addition of CNTs could resulted in extra crosslinking sites in addition to the usual urethane linkages.[14] However, to the best of our knowledge, the effect of CNTs on the reaction has not been systematically studied.

The purpose of this study was to investigate the influence of CNTs on the PU reactive foaming. The final properties of similar foams were reported elsewhere.[12, 14] Here, we provide a detailed analysis of the evolution of the polyurethane reaction by *in-situ* infrared spectroscopy and rheology experiments comparing the effects of chemically inert CNTs and reactive CNTs bearing oxygen-containing groups on the surface.

Experimental Part

Materials

The isocyanate was a methylene diphenyl diisocyanate (MDI), Voranate M2940 (NCO content: 31.4 wt.-%) and the polyol was a polyether based triol, Voranol 6150 (OH value: 27 mgKOH/g), both from Dow Plastics. The following additives were also used: a polyether based triol Voranol CP1421 (OH value: 31 mgKOH/g), used as a cell-opener, FASCAT 4202 (dibutyltin dilaurate, Arkema Inc) which is a tin catalyst

required for the gelling reaction, both TEDA-L33B (33% triethylendiamine in 1,4-butanediol) and NIAX catalyst E-A-1 (23% bis(2-dimethylaminoethyl)ether in dipropylene glycol) are tertiary amine catalysts that promote the isocyanate-water blowing reaction of the isocyanate and the polyol and balance the tin catalyst, DEOA (85 wt.-% diethanolamine in water) is a cross-linking chain extender, SH 209 is a silicone surfactant and distilled water as blowing agent. Polyurethane foam formulation is traditionally referred in parts by weight per 100 parts of polyol (phpp). The isocyanate index of the foams was set at 100. Formulation details are listed in **Table 1**.

Table 1.

Aligned multi-wall carbon nanotubes (CNTs) were grown by the chemical vapour deposition (CVD) injection method based on the decomposition of a ferrocene-toluene vapour (3 wt.-% of ferrocene in toluene). The synthesis was carried out at 760 ºC under an inert argon atmosphere and the solution injected at 5 mL/h. As-produced, the diameters are around 40 nm and the length is 160 μm (data not shown).[14, 18] Afterwards, these nanotubes were chemically-treated with a 3:1 concentrated sulphuric–nitric acid mixture and refluxed at 120 ºC for 30 min, and then filtered and washed with distilled water until neutral pH. The functionalised CNTs were then dried at 120 ºC and stored in a sealed container under vacuum prior to use to avoid possible effects of chemisorbed water on the reaction.

Functionalised CNTs have oxygen-containing groups, especially hydroxyl, carbonyl and carboxylic functionalities, on their surface.[14, 19] Both as-produced and functionalised CNTs are cut during subsequent oxidative and shear processes to a few microns.[20, 21]

Sample preparation

Foams were prepared using a two step procedure. Two loading fractions of both as-produced (CNTs) and functionalised CNTs (f-CNTs) were selected for this study 0.1 and 0.5 phpp which correspond to approximately 0.06 and 0.33 wt.-% of the final foam. First, a fixed amount of CNTs was added into the polyol (Voranol 6150). The mixture was initially sonicated for 10 min with an ultrasonication probe (Sonics VibraCell) in a water/ice bath, and was then stirred under high shear at 2400 rpm for 6 hours. Subsequently, the surfactant, catalysts and distilled water were added to the filler-polyol mixture and stirred at 2400 rpm for 3 min. Finally, the isocyanate was added and mixed for 20 sec before foaming occurred in an open cylindrical mould. The samples nomenclature is as follows: the number indicates the quantity of CNTs, i.e. PU/0, PU/0.1 and PU/0.5. The samples marked with an f correspond to f-CNTs.

Sample characterisation

The viscosity of the polyol-CNTs dispersions was measured using a TA Instruments Advanced Rheometer AR1000. The geometry used was a stainless steel corrugated parallel plate with a diameter of 20 mm. The gap was fixed to 3 mm and the measurements were recorded in frequency from 0.01 to 10 Hz at 21ºC and at an oscillation stress of 6.4 Pa. The results are averaged over three different samples. The standard error for each set of samples was less than 1%.

The structure of the foams was qualitatively examined using a Philips XL30 environmental scanning electron microscopy (ESEM) at 15kV. Cross-sections of the samples were cryo-fractured perpendicular to the foaming direction and the fracture surface was sputter coated with gold/palladium.

Infrared spectra were obtained using a Perkin-Elmer Spectrum One FT-IR Spectrometer fitted with an Attenuated Total Reflectance (ATR) accessory under unforced conditions. The reactive mixture was placed in direct contact with the diamond crystal immediately after the isocyanate was mixed with the rest of the ingredients. Measurements were collected at 8 cm^{-1} resolution and co-adding 6 scans per spectrum. The scanning time per spectrum was 2 min and the reaction was followed for 60 min. A background file was recorded prior to each run at 4 cm^{-1} resolution co-adding 6 scans per spectrum. A total of 5 spectra per sample were recorded and analysed to obtain statistically-relevant data.

A Rapra Scanning Vibrating Needle Curemeter (SVNC) was used to obtain the cure profiles of polyurethane foams.[22] This equipment simultaneously measures the elastic and viscous response of the system using a vibrating needle by measuring both the resonant frequency and amplitude. The mechanism consists on a carbon needle set to vibrate at an adjustable frequency in an electrically driven vibrator. The back electromotive force of the vibrator gives a measure of the vibration amplitude, and the vibration frequency is computer-controlled to maintain the maximum amplitude. As the viscosity of the curing liquid increases, it damps the vibration of the probe which is seen as a decrease on the amplitude. Once the material passes through the gel point, it starts to develop elastic properties which results in a shift of the resonance to higher frequencies. The output data is presented as the vibrating frequency, which is related to the storage modulus (G'), and the vibrating amplitude, which is related to the viscosity (before gelation) and the loss modulus (G'', after gelation).[22-24] The experimental measurements were carried out by centring the needle, a 50 cm long carbon fibre, in the middle of the mould and then, connecting it to the vibrator head. The process was continuously monitored over 2 h and the results are the average of at least three

different foam samples. The experimental error for each set of samples was around 10 % ascribed to small-scale laboratory sample preparation and mixing, and vibrating needle positioning.

Results and Discussion

The foaming evolution of polyurethane foams involves the interplay of several physical phenomena such as surface tension and bulk viscosity[25] of the initial reactants which determine the final cellular microstructure of the system. Therefore, we initially studied the rheological behaviour of the polyol/CNT dispersions. **Figure 1** shows the dependence of the complex viscosity with the angular frequency for 0, 0.1, 0.5, 0.1f, 0.5f phpp CNT mixtures. As expected, the addition of CNT resulted in an increase of the complex viscosity and a dependency of frequency with loading fraction.[26-28] We observed a change on the rheology behaviour from a Newtonian fluid to a non-linear power-law fluid with yield stress. This change has been associated to the formation of an interconnected structure of carbon nanotubes that restrains the motion of the polymer chains, hence indicating the existence of a rheological percolation network.[26] The functionalisation of the CNTs produced a less marked change of the complex viscosity as compared to as-produced CNTs, which was attributed to a shorter nanotube length as a result of the aggressive acid treatment and better dispersion state.[29] According to Doi and Edwards theory,[30, 31] the rheology of rods in solution is strongly dependent on rod concentration and aspect ratio. Functionalised CNT present a low aspect ratio and, hence, their solutions would correspond to a dilute or semidilute regime where nanotube interactions are small.

Figure 1

The rheological behaviour described above was further analysed by the Herschel-Bulkley model (**Equation 1**). This model describes a non-linear power-law fluid with a yield stress and is valid for a wide range of dispersions, emulsions and foams.[32] The model has also been applied to CNT dispersions[32-34] and, in particular, to polyol dispersions:[33]

$$\eta^* = \frac{\tau_0}{\omega} + k\omega^{n-1} \qquad (1)$$

where η^* is the complex viscosity, ω the angular frequency, τ_0 the yield stress, k the consistency index and n is the flow behaviour index. If $n > 1$, the fluid shows a shear-thickening behaviour; for $n = 1$, it behaves as a Newtonian fluid with a yield stress term added to it (or Bingham fluid); and for $n < 1$, the fluid shows a shear-thinning behaviour. **Table 2** summarises the parameters and quality of fit (reduced χ^2) obtained for the data applying the Herschel-Bulkley model. The fitting parameters obtained confirmed the Newtonian behaviour of the neat polyol and the quasi-linear behaviour of the low loading fraction mixtures, 0.1 phpp CNT and f-CNT. Meanwhile, the fitting parameters of both polyol/0.5 and polyol/0.5f mixtures clearly presented the shear-thinning behaviour (n<1) of the Herschel-Bulkley fluid. The main difference between these two mixtures was the yield stress, as produced CNT showed a large yield stress indicative of strong CNT interactions and possible CNT network.

Table 2

Shear-rheology of CNT mixtures, described as Herschel–Bulkley fluids, have been related to the elongational viscosity of the mixtures,[34] which can provide information

on film stability to capillary pinching and breaking. The study suggested that the hydrodynamic interactions of CNTs in the fluid slowed down the self-thinning process, understood as the process by which a fluid thread thins down and breaks up under no external forces, and led to lower film instabilities. Therefore, according to the rheological data, foam nanocomposites would present larger film stability and, hence, closed cell content compared to the unfilled sample. However, SEM inspection of the samples did not reveal significant differences on the openness/closeness of the cells (**Figure 2**) which could suggest that the CNT had a destabilising effect on the cell walls through a bridging-dewetting mechanism.[35] Similar results were observed by microradiology to occur towards the end of the foaming process of a reactive open-cell silicone foam.[17] Nevertheless, cell opening is a complex mechanism and both non-dewetting[36] and dewetting[37] effects of nanoclays and carbon nanofibres have been reported in literature. The cell density and sizes appeared to be comparable and, hence, no nucleation effect was observed from the CNTs.[14] Close inspection of the polymeric matrix revealed a good dispersion of CNTs throughout the sample, in both the walls, and particularly the struts of the cellular structure.

Figure 2

Formation of a flexible polyurethane foam is a complex process involving many ingredients and several competing reactions.[3] Hence, infrared spectroscopy is particularly useful to analyse the time-related aspects of foam evolution and morphology development.[1, 5-7] In polyurethane foams, these analyses are carried out by studying four particular regions: (1) the NH stretching region, 3500-3200 cm^{-1}; (2) the amide I region or carbonyl region, 1800-1600 cm^{-1}; (3) the isocyanate absorbance band

at approximately 2300 cm^{-1}; and (4) the amide II region, below 1600 cm^{-1}. Here, the NH stretching and the amide II regions were not considered due to variations on the extinction coefficient with hydrogen bonding and the complex nature of the absorbance peaks, respectively.[6] To compensate for the large density change of the systems, the spectra were normalised by the intensity of an internal reference band that remained constant during the reaction (generally 2970 cm^{-1} corresponding to CH stretch).[1, 5] **Figure 3** shows representative spectra obtained at different reaction times showing the evolution of the carbonyl region and the isocyanate absorbance band.

Figure 3

The decrease in the isocyanate absorbance as a function of reaction time is related to the reactions of the isocyanate with both the polyol and water to form urethane and urea groups, respectively. Hence, this band is used to calculate the extent of the reaction as:

$$p_{NCO} = 1 - \frac{A_{NCO}}{A_0} \qquad (2)$$

where A_{NCO} is the ratio of the integrated absorbance of the isocyanate and that of the internal standard, and A_0 is at zero reaction time. The isocyanate conversion of the foams showed clear differences due to the presence of CNTs at the early stages of the process (**Figure 4**). Isocyanate conversion rate, taken as the slope of the curves up to microphase separation (discussed below), decreased as a function of CNT loading fraction (**Figure 4, inset**). Hence, filled samples presented a lower reaction rate than the unfilled sample at the early stages of the reaction. We were expecting that the presence of OH-bearing groups on the functionalised CNT surface would accelerate the

isocyanate conversion; however, we observed the same conversion trend on as-produced and functionalised CNT samples. Such trend suggested that the isocyanate conversion rate was dominated by the CNT content and not by the functionality. Therefore, the isocyanate reaction was mainly governed by kinetic effects due to the initial viscosities of the mixtures and the low mobility of the molecular chains.[38, 39] Similar argument on the importance of the kinetic effects have been highlighted by Camberlin and Pascault[38] on linear PU formulations and Li *et al.*[39, 40] on segmented PU formulations. An analogous delay in the foaming process was qualitatively observed in both PU and silicone reactive foams filled with carbon based nanofillers.[11, 14] However, the opposite behaviour has been reported on 5 and 10 wt.-% montmorillonite/PU foams[16] due to the presence of swollen water within the nanoclay layers.

Figure 4

As the intensity of the isocyanate band decreased, the intensities of the bands related to the carbonyl stretch increased in the amide I mode. The intensities of these bands are extremely sensitive to changes in the order of hydrogen bonded carbonyl groups,[41] as well as the strength and specificity of the hydrogen bonds formed.[7] **Figure 5** shows the infrared spectra collected at the initial stages of the reaction in the carbonyl region for PU/0.1 sample. Four different bands corresponding to free urethane (1728 cm^{-1}), free urea (1710 cm^{-1}), monodentate urea (1670 cm^{-1}) and bidentante urea (1640 cm^{-1})[6, 7] can be observed. The vibrations at 1670 and 1640 cm^{-1} are assigned to disordered and ordered hydrogen-bonded urea groups, respectively.

Figure 5

The urea groups produced during the blowing reaction start to segregate and associate via the formation of hydrogen bonds.[8] Hence, the formation of the hydrogen-bonded urea, or bidentate urea, is considered as the onset of microphase separation (microphase separation time, MST) of the segmented block copolymer.[1] Following Elwell *et al.*,[1] the MST was established by normalising the bidentate urea absorbance ($[>C=O]_b$) by the isocyanate conversion, to remove concentration effects, and was then taken at the point where the concentration of hydrogen-bonded groups increased sharply (**Figure 6**). Previous works observed that the MST for slabstock foams occurred at a critical isocyanate conversion of 0.55 ± 0.05,[5, 6, 8] which is similar to the value obtained in this study for unfilled and as-produced CNT samples (**Table 3**). However, functionalised CNTs produced a clear shift of the MST towards lower values of critical isocyanate conversion. This result suggested that the presence of hydroxyl and carboxyl groups on the CNT surface triggered the formation of hydrogen-bonded ureas at a lower conversion of isocyanate.

Figure 6

Table 3

We finally analysed the rheological behaviour of the evolving system. *In-situ* measurements of modulus and viscosity development during reactive foaming is a difficult task due to the exothermic nature of the reaction and its rapid volume expansion.[9] However, some attempts can be found in the literature using both a vane

rheometer and a flooded parallel plate dynamic rheometer.[1, 4, 6, 9, 42] These studies have divided the rheological behaviour of the evolving polyurethane foams into four regions (**Scheme 2**):[4, 9, 43] 1) initial bubble nucleation and growth, 2) evolution of the bubbles and formation of urethane and soluble urea leading to the onset of microphase separation 3) stiffening of the polymer and cell opening; and 4) final chemical gelation or curing. In this study, we used a scanning vibrating needle curemeter (SVNC) to obtain qualitative trends of the rheological changes of foaming and curing (**Figure 7**).[44]

Scheme 2

Figure 7

The first region is estimated to last approximately 30s and could not be captured due to the experimental delay while loading the sample in the detector. Similar problem has been reported elsewhere, however it is assumed that the viscosity in this region corresponds to the initial viscosity of the dispersions.[1, 9] In this first region, the air bubbles dissolved within the foaming mixture during mixing act as nucleating points for the evolving CO_2 generated by the reaction between isocyanate and water.[9]

The second region (Zone 2, Figure 7 insets) is characterised by the expansion of the bubbles due to the continued generation of CO_2 gas leading to the development of a packed bubble network. The end of this region has been associated to the onset of microphase separation (MST) of the urea hard segment domains.[1] As previously mentioned, the MST occurs as the degree of polymerisation of the hard segments reaches a critical value and the system undergoes a disordered-ordered transition.[1] At this point, flexible PU foam phase separate by spinodal decomposition, therefore a

bicontinuos morphology (of a polyurea dominated “hard phase” and a polyether dominated “soft phase”) forms at the start of this process, with each phase becoming less phase-mixed as the process proceeds. We observed that the onset of microphase separation, previously established by FTIR, matched the points where the amplitude traces stopped their decrease in a relative minimum. To explain this coincidence we should remember that the amplitude is inversely proportional to the material damping characteristics, which depend on the crosslink density and, thus, on the evolution of the urea hard segments.

Above the MST (Zone 3, Figure 7 insets), the amplitude or loss modulus levelled while the frequency or storage modulus increased as the polymerisation proceeded. The rise in the polymer modulus is a consequence of the microphase separation, which is intercepted and vitrified by the urea rich phase, triggering the cell opening.[34] Cell opening has previously been observed to occur at a critical degree of isocyanate conversion of about 70 %.[1, 5] The time length of this region is clearly distinguished in the amplitude response with all samples, except PU/0.5f, showing similar duration. The MST shift observed by FTIR of the f-CNTs could account for this difference on the region duration.

The last region (Zone 4, Figure 7 insets) is related to the final curing of the foams. The storage modulus continues to increase at a slow pace until it stabilises once the vitrification and formation of covalent cross-links of the hard segments is completed.[1] In our systems, the storage modulus of PU/0, PU/0.1, PU/0.1f agreed within error (frequency~115 Hz) while PU/0.5, PU/0.5f, reached a much higher value (~135 and ~150 Hz, respectively). This result suggested that while the incorporation of 0.5 phpp CNT (or 0.33 wt.-% CNT) was sufficient to reinforce the matrix, the addition of 0.1 phpp CNT (or 0.06 wt.-% CNT) was not. This non-reinforcing effect at low loading

fractions has also been reported on a similar PU foam filled with 0.1 wt.-% CVD-CNT and was associated to the relatively high defect concentration of CVD grown CNTs.[12] The larger storage modulus of PU/0.5f compared to PU/0.5 and its upward trend suggested changes in the final hard segment content and their interconnectivity.[6] Previous works on phase segregation in polyurethanes had shown a relationship between the equilibrium time and the system viscosity, hard segment mobility and hard segment interactions.[38-40] This result agreed with the early development of the bidentate urea observed on the FTIR.

Conclusion

The study of the foaming evolution of PU nanocomposite foams was carried out *in-situ* by two different techniques: rheology and FT-IR spectroscopy, and was evaluated as a function of CNT loading fraction and surface functionality. First, the rheological behaviour of polyol-CNT dispersions was studied to understand the effect of the initial viscosity on the subsequent foaming process and cellular morphology. Kinetic effects were observed to play a dominant role on the rate of the reaction at the early stages, due to a reduction on chain mobility. Moreover, the onset of the microphase separation was influenced by the presence of functional groups on the CNT surface. These differences on the microphase separation would be a necessary though not sufficient indication of changes on the hard and soft segments, signifying the potential to manipulate the polyurethane morphology. Further investigations will be carried out to analyse precisely the effects of CNTs and CNT functionalities on the morphological changes by small-angle x-ray scattering and AFM. The qualitative results obtained of the rheological changes occurred during foaming were well correlated with those in the FT-IR spectroscopy.

Acknowledgements: The authors gratefully acknowledge the financial support of the *Spanish Ministry of Science and Innovation* (MICINN) through project MAT 2010-18749 and the *7th Framework Program of E.U.* through HARCANA (NMP3-LA-2008-213277). RV and MMB also acknowledge the *Ramon y Cajal* and FPI programmes from MICINN, respectively.

Received: ((will be filled in by the editorial staff)); Revised: ((will be filled in by the editorial staff)); Published online: ((will be filled in by the editorial staff));
DOI: ((will be filled in by the editorial staff))

Keywords: carbon nanotubes; polymerisation; polyurethane foams; infrared spectroscopy

[1] M. J. Elwell, A. J. Ryan, H. J. M. Grunbauer, H. C. VanLieshout, *Macromolecules* **1996**, *29*, 2960.

[2] J. H. Saunders, R. H. Hansen, "The Mechanism of Foam Formation", in *Plastics Foams*, K.C. Frisch and J.H. Saunders, Eds., Marcel Dekker, New York, 1972.

[3] D. Klempner, V. Sendijarevic, "*Handbook of polymeric foams and foam technology"*, Hanser Publishers, 2004.

[4] R. A. Neff, C. W. Macosko, *Rheol. Acta* **1996**, *35*, 656.

[5] M. J. Elwell, A. J. Ryan, H. J. M. Grunbauer, H. C. VanLieshout, *Polymer* **1996**, *37*, 1353.

[6] W. Li, A. J. Ryan, I. K. Meier, *Macromolecules* **2002**, *35*, 6306.

[7] A. M. Heintz, D. J. Duffy, C. M. Nelson, Y. Hua, S. L. Hsu, W. Suen, C. W. Paul, *Macromolecules* **2005**, *38*, 9192.

[8] L. D. Artavia, C. W. Macosko, *Journal of Cellular Plastics* **1990**, *26*, 490.

[9] E. Mora, L. D. Artavia, C. W. Macosko, *J. Rheol.* **1991**, *35*, 921.

[10] H. Z. Feng, X. L. Wang, H. S. Xia, *Acta Polym Sin* **2009**, 953.

[11] R. Verdejo, C. Saiz-Arroyo, J. Carretero-Gonzalez, F. Barroso-Bujans, M. A. Rodriguez-Perez, M. A. Lopez-Manchado, *Eur. Polym. J.* **2008**, *44*, 2790.

[12] R. Verdejo, G. Jell, L. Safinia, A. Bismarck, M. M. Stevens, M. S. P. Shaffer, *Journal of Biomedical Materials Research Part A* **2009**, *88A*, 65.

[13] R. Verdejo, F. Barroso-Bujans, M. A. Rodriguez-Perez, J. A. de Saja, M. Arroyo, M. A. Lopez-Manchado, *J Mater Chem* **2008**, *18*, 3933.

[14] R. Verdejo, R. Stampfli, M. Alvarez-Lainez, S. Mourad, M. A. Rodriguez-Perez, P. A. Bruhwiler, M. Shaffer, *Compos Sci Technol* **2009**, *69*, 1564.

[15] T. U. Patro, G. Harikrishnan, A. Misra, D. V. Khakhar, *Polym. Eng. Sci.* **2008**, *48*, 1778.

[16] A. N. Wilkinson, N. H. Fithriyah, J. L. Stanford, D. Suckley, *Macromol. Symp.* **2007**, *256*, 65.

[17] R. Verdejo, F. J. Tapiador, L. Helfen, M. M. Bernal, N. Bitinis, M. A. Lopez-Manchado, *PCCP* **2009**, *11*, 10860.

[18] C. Singh, M. S. P. Shaffer, A. H. Windle, *Carbon* **2003**, *41*, 359.

[19] R. Verdejo, S. Lamoriniere, B. Cottam, A. Bismarck, M. Shaffer, *Chem. Commun.* **2007**, 513.

[20] J. Liu, A. G. Rinzler, H. Dai, J. H. Hafner, R. K. Bradley, P. J. Boul, A. Lu, T. Iverson, K. Shelimov, C. B. Huffman, F. Rodriguez-Macias, Y.-S. Shon, T. R. Lee, D. T. Colbert, R. E. Smalley, *Science* **1998**, *280*, 1253.

[21] K. L. Lu, R. M. Lago, Y. K. Chen, M. L. H. Green, P. J. F. Harris, S. C. Tsang, *Carbon* **1996**, *34*, 814.

[22] B. G. Willoughby, K. W. Scott, "Understanding Cure with the Scanning Vibrating Needle Curemeter (Scanning VNC) ", R.T. Limited, Ed., Shawbury, 1991.

[23] D. J. Allwright, B. G. Willoughby, "Towards a Mathematical Model of the Scanning Vibrating Needle Curemeter", in *Technical Meeting of the Rubber Division*, American Chemical Society, San Francisco, 2003, p. 74/1.

[24] D. J. Allwright, "The Scanning Vibrating Needle Curemeter", 40th European Study Group with Industry, RAPRA Technology, http://www.smithinst.ac.uk/Projects/ESGI40/ESGI40-RAPRA/Report/Curemeter.pdf, 2010.

[25] R. K. Prud'homme, S. A. Khan, "Foams: Theory, Measurements and Applications", CRC Press, New York, 1996.

[26] S. Bose, A. R. Bhattacharyya, A. R. Kulkarni, P. Pötschke, *Compos Sci Technol* **2009**, *69*, 365.

[27] Y. Y. Huang, S. V. Ahir, E. M. Terentjev, *Phys. Rev. B* **2006**, *73*.

[28] Q. Zhang, S. Rastogi, D. Chen, D. Lippits, P. J. Lemstra, *Carbon* **2006**, *44*, 778.

[29] J. H. Xu, S. Chatterjee, K. W. Koelling, Y. R. Wang, S. E. Bechtel, *Rheologica Acta* **2005**, *44*, 537.

[30] M. Doi, S. F. Edwards, "*The Theory of Polymer Dynamics"*, Oxford Press, London, 1986.

[31] S. Marceau, P. Dubois, R. Fulchiron, P. Cassagnau, *Macromolecules* **2009**, *42*, 1433.

[32] I. A. Kinloch, S. A. Roberts, A. H. Windle, *Polymer* **2002**, *43*, 7483.

[33] H. S. Xia, M. Song, *Soft Matter* **2005**, *1*, 386.

[34] M. K. Tiwari, A. V. Bazilevsky, A. L. Yarin, C. M. Megaridis, *Rheologica Acta* **2009**, *48*, 597.

[35] B. P. Binks, *Current Opinion in Colloid and Interface Science* **2002**, *7*, 21.

[36] G. Harikrishnan, S. N. Singh, E. Kiesel, C. W. Macosko, *Polymer* **2010**, *51*, 3349.

[37] G. Harikrishnan, T. U. Patro, D. V. Khakhar, *Industrial and Engineering Chemistry Research* **2006**, *45*, 7126.

[38] Y. Camberlin, J. P. Pascault, *Journal of Polymer Science, Part B: Polymer Physics* **1984**, *22*, 1835.

[39] Y. Li, W. Kang, J. O. Stoffer, B. Chu, *Macromolecules* **1994**, *27*, 612.

[40] Y. Li, Z. Ren, M. Zhao, H. Yang, B. Chu, *Macromolecules* **1993**, *26*, 612.

[41] M. M. Coleman, K. H. Lee, D. J. Skrovanek, P. C. Painter, *Macromolecules* **1986**, *19*, 2149.

[42] X. D. Zhang, D. W. Giles, V. H. Barocas, K. Yasunaga, C. W. Macosko, *J. Rheol.* **1998**, *42*, 871.

[43] A. P. Singh, M. Bhattacharya, *Polym. Eng. Sci.* **2004**, *44*, 1977.

[44] S. A. Jones, K. W. Scott, B. G. Willoughby, E. A. Sheard, *Journal of Cellular Plastics* **2002**, *38*, 285.

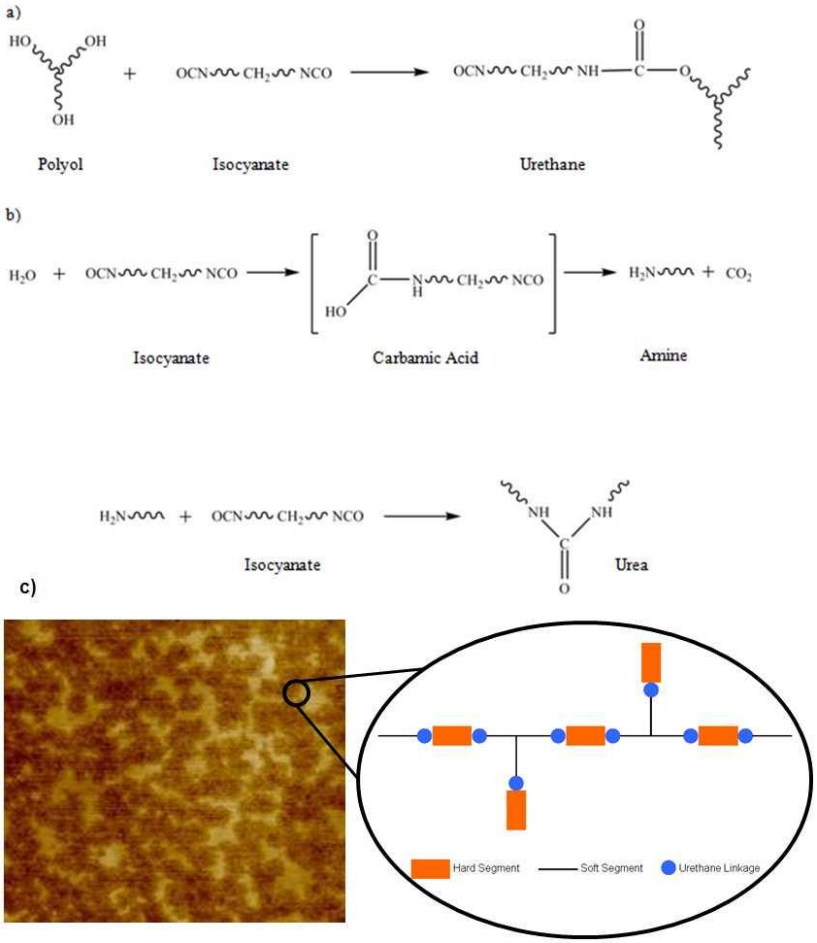

Scheme 1. Chemistry of PU foams: a) Gelling reaction and b) Blowing reaction. c) AFM image (3×3 μm) and diagram showing the segmented block copoly(ether-urethane urea) microdomains formed in polyurethanes.

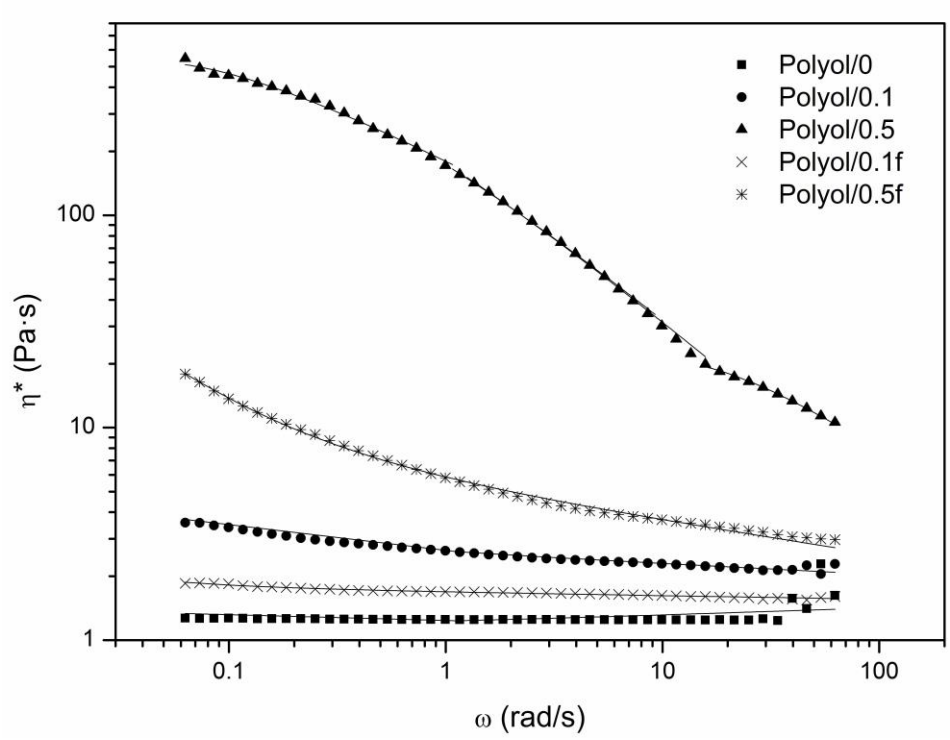

Figure 1. Representative curves of the complex viscosity versus angular frequency of the polyol/CNT dispersions. The solid lines are the fit to the Herschel-Bulkley theory.

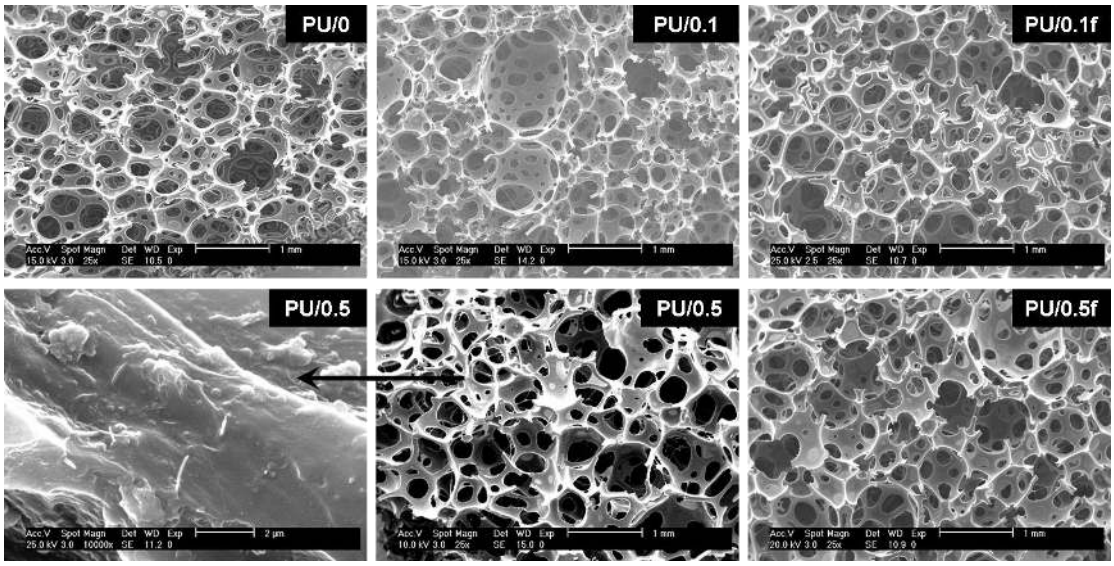

Figure 2. Representative SEM images of the samples at low magnification (scale bar 1 mm) and CNT dispersion in PU/0.5 sample at high magnification.

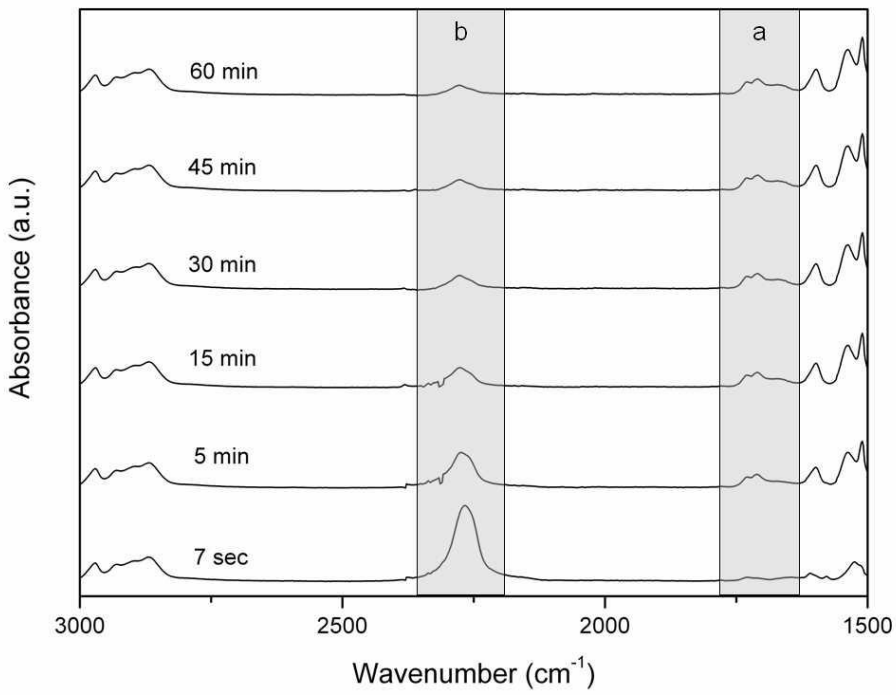

Figure 3. Infrared spectra of PU/0 sample at different reaction times illustrating the evolution of (a) the carbonyl region and (b) the isocyanate absorbance band.

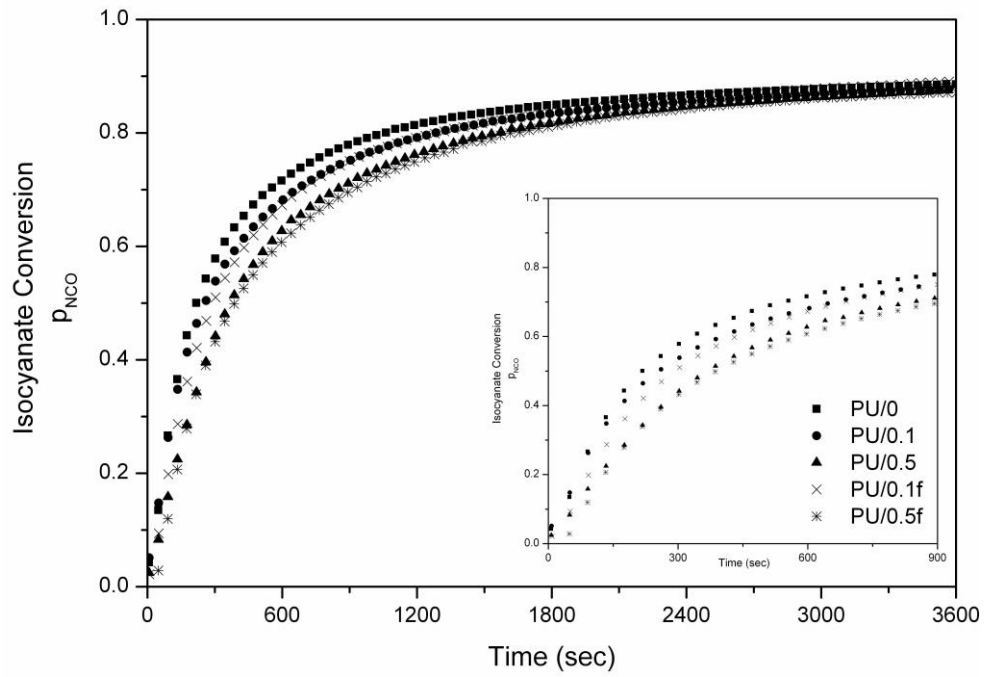

Figure 4. Isocyanate conversion as a function of time of the PU nanocomposite foams under study. The inset shows the isocyanate conversion at the early stages of the reaction (up to 900 sec).

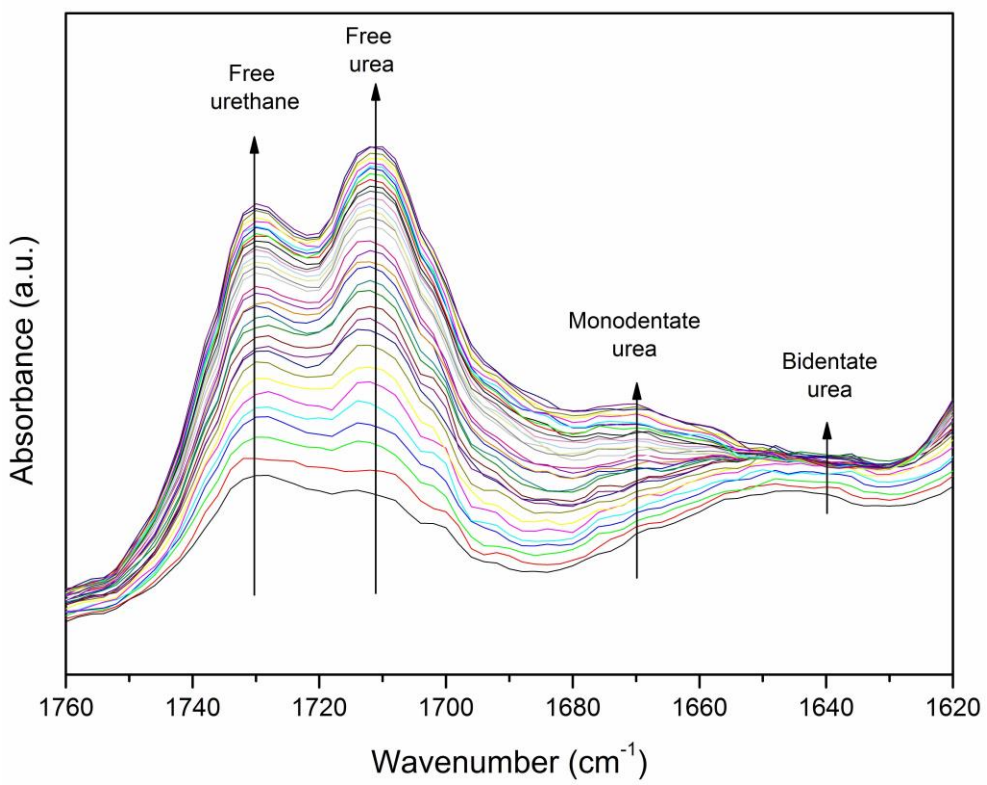

Figure 5. Evolution of the amide I region (1760-1620cm^{-1}) during the first 180 sec of the reaction for the PU/0.1 sample.

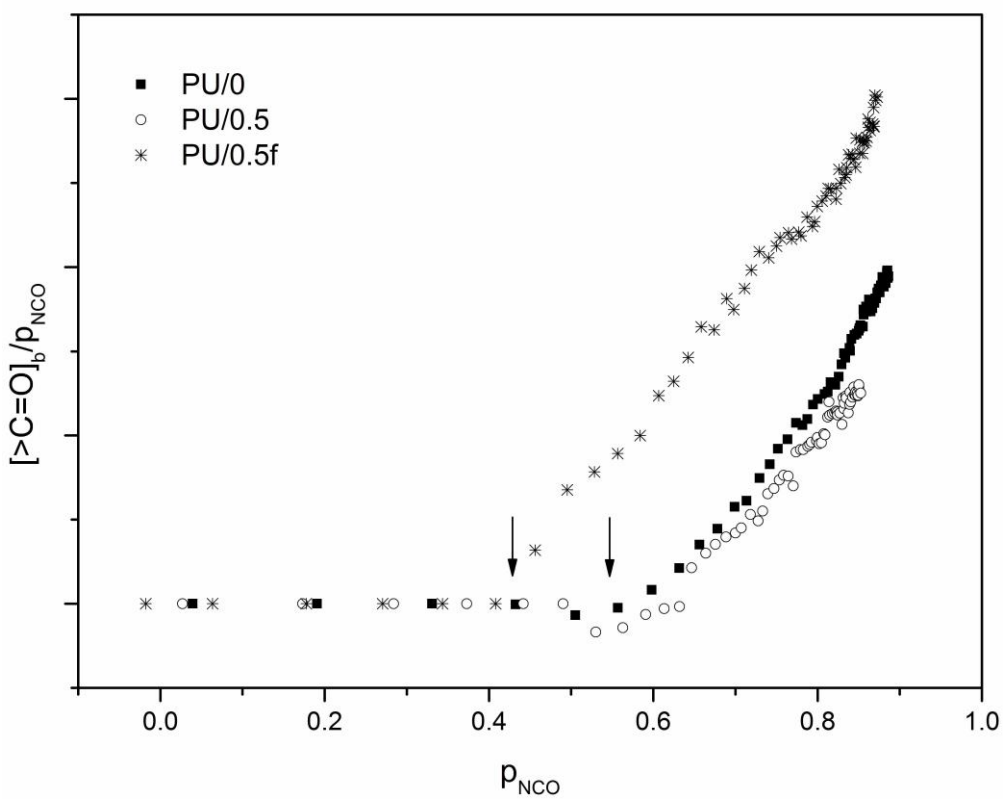

Figure 6. Ratio of $[>C=O]_b/p_{NCO}$ as a function of p_{NCO} for PU/0, PU/0.5 and PU/0.5f. The MST is marked with arrows for the different samples.

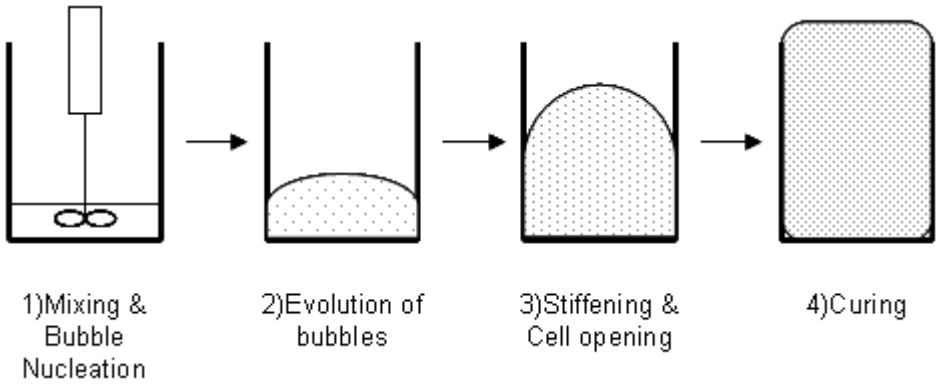

Scheme 2. Schematic representation showing the stages observed in flexible PU foaming.

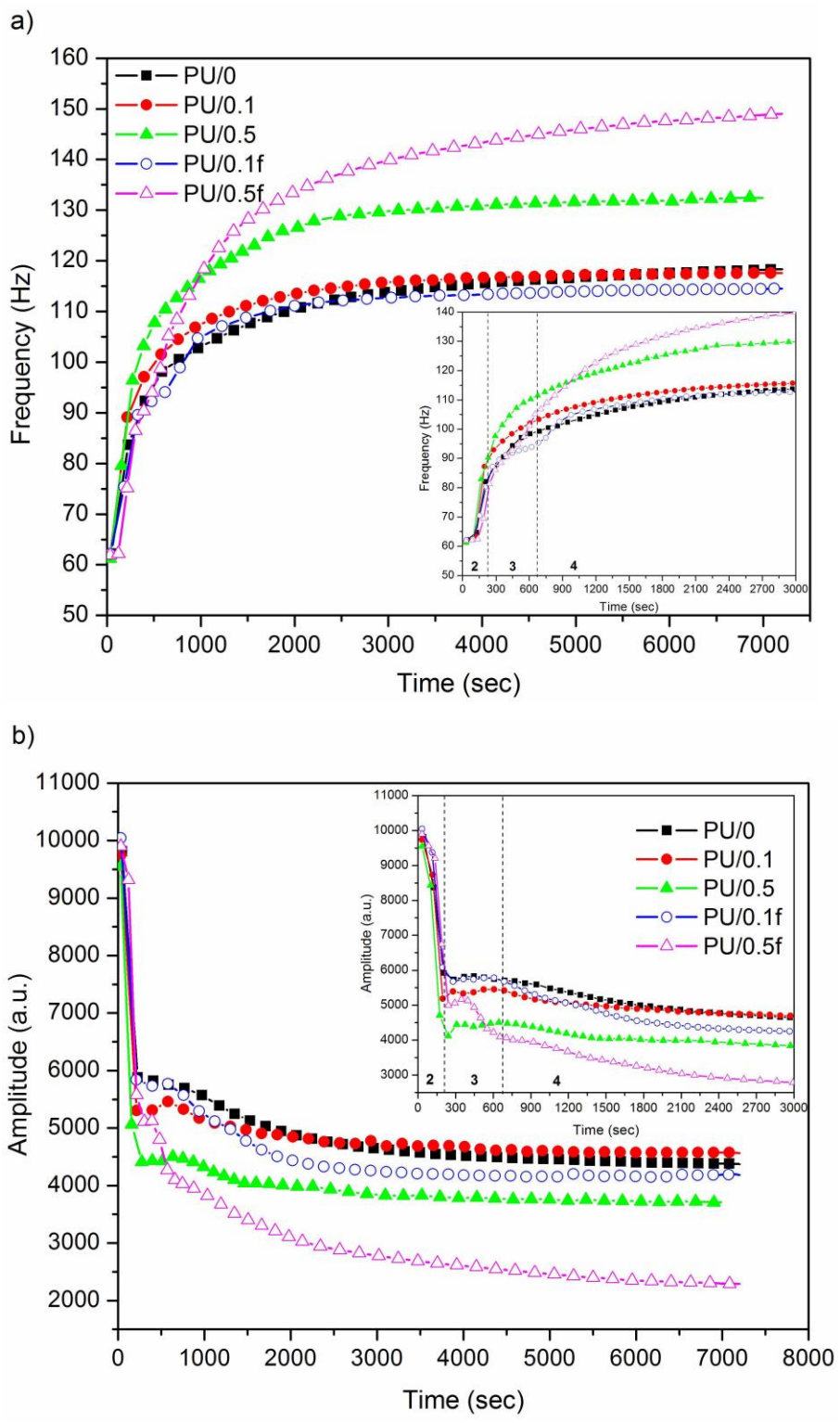

Figure 7. Representative data sets of (a) the frequency, or elastic behaviour, and (b) the amplitude, or damping behaviour, for PU/0, PU/01, PU/0.1f, PU/0.5 and PU/0.5f samples. The insets show a close up of the early stages of the evolution and the vertical lines mark the different foaming regions.

Tables:

Table 1. Formulation used to prepare the polyurethane foams in this study.

Materials	**Voranol 6150**	**Voranol CP1421**	**Voranate M2940**	**DEOA**	**NIAX E-A-1**	**FASCAT 4202**	**TEDA L33B**	**Silicone SH209**	**Water**
PU (phpp[a])	100	4	43.4	0.8	0.1	0.05	0.25	0.4	2.2

[a] parts by weight per 100 parts of polyol

Table 2. Parameters and quality of fit of the Herschel-Bulkley model for the CNTs polyol dispersions

Samples	τ_0 **(Pa)**	k **(Pa·s^n)**	n	**Quality of fit** χ^2
Polyol/0	0	1.25	0.99	$3.4 \cdot 10^{-6}$
Polyol/0.1	~0	2.60	0.94	$4.3 \cdot 10^{-4}$
Polyol/0.5	195.95	22.27	0.71	1.9
Polyol/0.1f	~0	1.66	0.97	$1.1 \cdot 10^{-3}$
Polyol/0.5f	0.62	5.24	0.84	$1.9 \cdot 10^{-2}$

Table 3. Conversion of isocyanate groups (p_{NCO}) at the onset of bidentate urea formation

Sample	**p_{NCO} at onset**
PU/0	0.61±0.06
PU/0.1	0.58±0.01
PU/0.5	0.60±0.09
PU/0.1f	0.54±0.04
PU/0.5f	0.45±0.07

The effect of both as-produced and functionalised CNTs on the polymerisation of water-blown PU foams is studied by *in-situ* FT-IR spectroscopy and viscoelastic properties. Kinetic effects were observed to play a dominant role on the rate of the reaction at the early stages.

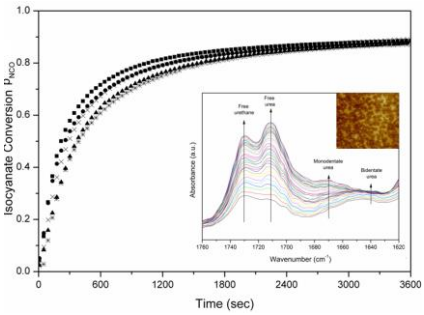

M. Mar Bernal, Miguel Angel Lopez-Manchado, Raquel Verdejo*

In-Situ Foaming Evolution of Flexible Polyurethane Foam Nanocomposites